ELECTROMAGNETIC MODELING OF A RESISTIVE SUPERCONDUCTING FAULT CURRENT LIMITER

Eduardo S. Motta[1], Rubens de Andrade Jr[2], Richard M. Stephan[2]
[1]INB Indústrias Nucleares do Brasil S.A., Rodovia Presidente Dutra, km 330, 27555-000, Resende, RJ, BRAZIL
eduardomotta@inb.gov.br
[2]LASUP/UFRJ P.O. Box 68504 21945-970 Rio de Janeiro BRAZIL
rms@ufrj.br randrade@dee.ufrj.br

***Abstract* – The short circuit current level of interconnected power systems is constantly increasing. One of the solutions for this problem is the use of fault current limiters (FCL). Among different types of FCL, the resistive superconducting FCL (RSFCL) is one of the most promising technologies. In this work, the electromagnetic behavior and the power dissipation of a RSFCL is modeled. The results of this study are necessary for the design of reliable RSFCL. Analytical and numerical results are compared to ensure the correctness of the developed algorithm. With some modifications on the proposed algorithm, the influence of magnetic field and temperature variations are also modeled.**

***Keywords* – Fault current limiter, Superconductivity, Bean model.**

I. INTRODUCTION

With growing power systems and the introduction of new sources of energy and interconnections, the fault current levels increase. This increase demands the upgrade of protective circuit breakers, an expensive solution. As alternative, fault current limiters (FCL) can be employed [1]. Some types of FCL use power electronics.

A FCL must ideally:
- be invisible to the power system in normal conditions;
- limit short circuit currents to values that circuit breakers can open safely;
- present fast transition to the limiting state [2];
- present fast recovering after a fault [3];
- have low dissipation, high reliability, low maintenance and high capacity density.

High temperature superconductors (HTS) have these target characteristics. Among different types of superconductor FCL, the resistive superconducting fault current limiter (RSFCL) is promising.

One of the most important issues in RSFCL design is the power dissipation in order to establish the refrigeration needs. RSFCL works at temperatures below 100 K.

In this work, the electromagnetic behavior and the power dissipation of a long superconductor cylinder is deduced analytically using the Bean model [4]. The electromagnetic behavior is also determined numerically and the results are compared with the analytical ones, ensuring that the proposed algorithm is correct. With some modifications on the algorithm, the influence of magnetic field and temperature variations, which can not be obtained analytically, can also be modeled.

II. ELECTROMAGNETIC BEHAVIOR

The Bean model, used in this work in the analytical and first numerical simulation, is one of the simplest models that describe the superconductor behavior. There are two main premises in this model:
- every electromagnetic variation starts from outside to inside the superconductor [5],
- the current is not homogeneously distributed over the cross section of the superconductor, with no current flowing in some sectors and a constant current density in the rest [6].

A. Analytical Results

The analytical calculation for a long superconductor cylinder transporting the sinusoidal current $i(t)=I_{max}\sin(\omega t)$ was studied using cylindrical coordinates (Fig. 1).

This study is segmented in the following time intervals: $0<t< T/4$, $T/4<t<3T/4$, $3T/4<t<5T/4$, where $T=2\pi/\omega$ is the period of the supply current.

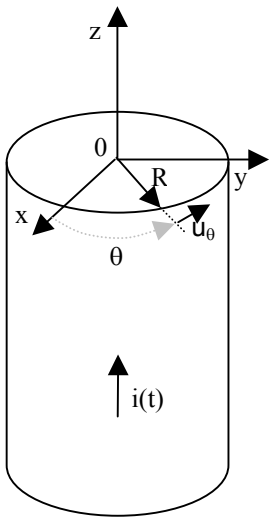

Fig.1. Superconductor cylinder transporting a sinusoidal current in the *z* direction. The cylinder, with *R* radius, is centered at *z* axis.

1) Interval (0<t<T/4) – This interval will study the establishment of the current and represents the transient period. Defining I_C the value of complete current penetration, it follows:

$$I_C = J_C \pi R^2 \quad (1)$$

For an instantaneous value *i(t)*, the current penetrates until a radius c(t) given by (2).

$$c(t) = R\sqrt{1 - \frac{i(t)}{I_C}} \tag{2}$$

The analytical solution for a solid cylinder is the same as for a tube with radius greater than the maximal penetration.

Using Amperè law, the magnetic field can be obtained and it has the same direction of the unitary vector u_θ. The solution is presented in (3).

$$r < c(t) \rightarrow B = 0$$

$$R > r > c(t) \rightarrow B = \frac{\mu_0 J_C}{2}\left(r - \frac{c(t)^2}{r}\right)$$

$$r > R \rightarrow B = \frac{\mu_0 J_C (R^2 - c(t)^2)}{2r} \tag{3}$$

The current variation implies in the magnetic field variation and, consequently, an electric field will appear in the superconductor. This electric field can be obtained from Faraday's law. This field has the same direction of the current density and its value is present in (4).

$$R > r > c(t) \rightarrow E(t,r) = \frac{\mu_0}{2\pi}\frac{di(t)}{dt}\ln\left(\frac{r}{c(t)}\right) \tag{4}$$

A graphical representation of the electromagnetic variables is present in Fig.2.

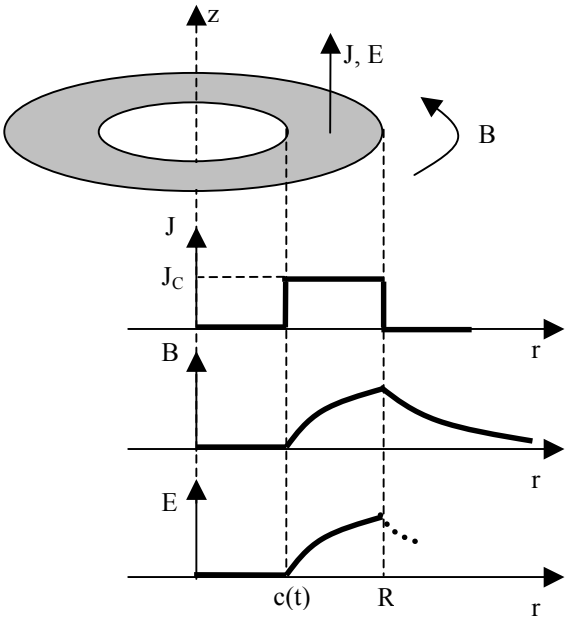

Fig.2. Distribution of the current density *J*, magnetic field *B* and electric field *E*, in a superconductor cylinder transporting a sinusoidal current *i(t)* (0<t<T/4).

Multiplying (4) by the constant current density J_C and integrating it in the cylinder volume, the power dissipation per unit of length *P(t)* can be obtained. For the sinusoidal current with angular frequency ω, the power loss per unit length is given by (5),

$$P(t) = 10^{-7} I_{\max}\omega\cos(\omega t).$$
$$\left[2\ln\left(\frac{\sqrt{-\frac{-I_C + I_{\max}\sin(\omega t)}{I_C}}\,I_C}{-I_C + I_{\max}\sin(\omega t)}\right)I_C - I_{\max}\sin(\omega t)\right] \tag{5}$$

and its mean value is given by (6).

$$P_{mean} = \frac{10^7}{\pi}\omega\left(\begin{array}{l} 2I_{\max}I_C\ln(I_C - I_{\max}) - 4I_{\max}I_C\ln\left(I_C\sqrt{\frac{1}{I_C}}\right) - 2I_C^2\ln(I_C - I_{\max}) \\ +4I_C^2\ln\left(I_C\sqrt{\frac{1}{I_C}}\right) + I_{\max}^2 - 2I_{\max}I_C \end{array}\right) \tag{6}$$

Figure 3 shows the power dissipation and its mean value for a sinusoidal current with effective value 50 A and 60 Hz, flowing in a superconductor cylinder with 3.6 mm radius and current density of 400 A/cm^2.

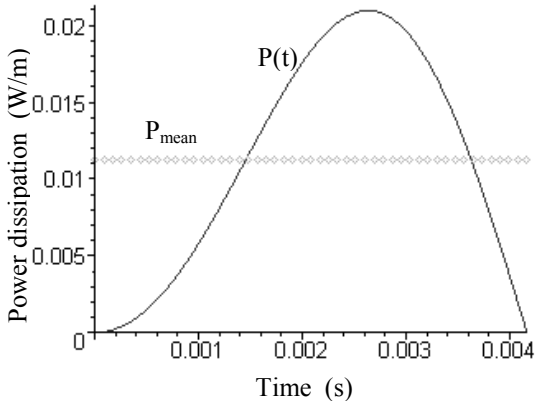

Fig.3. Power dissipation and its mean value for a sinusoidal current with effective value 50 A and 60 Hz, flowing in a superconductor cylinder with 3.6 mm radius and current density of 400 A/cm^2 (0<t<T/4).

2) Interval (T/4<t<3T/4). – With the decrease of the current value, a negative current density will appear at the outmost part of the cylinder as shown in Fig.4.

In this situation, the variation of the current density will occur up to a radius *c(t)*, now defined by (7).

$$c(t) = R\sqrt{1 - \frac{I_{\max}}{2I_C} + \frac{i(t)}{2I_C}} \tag{7}$$

There is no change in the magnetic field value for a radius smaller than *c(t)* and, consequently, no electric field and power dissipation.

Defining r_S as the radius that the current will penetrate at its peak value, the magnetic field is now defined by (8).

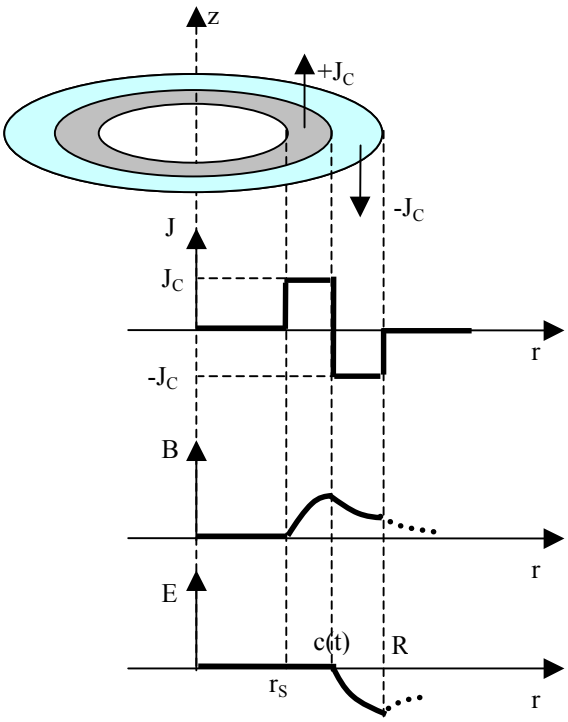

Fig.4. Distribution of the current density *J*, magnetic field *B* and electric field *E*, in a superconductor cylinder transporting a sinusoidal current *i(t)* (T/4<t<3T/4).

$$r < r_S \rightarrow B = 0$$

$$c(t) > r > r_S \rightarrow B = \frac{\mu_0 J_C}{2}\left(r - \frac{r_S^{\,2}}{r}\right)$$

$$R > r > c(t) \rightarrow B = \frac{\mu_0 i(t)}{2\pi r} - \frac{\mu_0 J_C}{2}\left(r - \frac{R^2}{r}\right) \quad (8)$$

Substituting (7) in (4), multiplying it by the constant current density $-J_C$ and integrating it in the cylinder volume, the power dissipation per unit of length *P(t)* can be obtained. For the sinusoidal current with angular frequency of ω, the power loss linear density is defined by (9).

$$P(t) = -10^{-7} I_{max}\omega\cos(\omega t).\left[\ln(2) I_C + 2\ln\left(\frac{\sqrt{\frac{2I_C - I_{max} + I_{max}\sin(\omega t)}{I_C}}\, I_C}{2I_C - I_{max} + I_{max}\sin(\omega t)}\right) I_C - I_{max} + I_{max}\sin(\omega t)\right] \quad (9)$$

The mean value of (9) is also defined by (6). Fig. 5 shows the power dissipation and its mean value for the same parameters used in Fig. 3.

Note that although the different power shapes presented in Figs. 3 and 5, they have the same mean value.

3) Interval (3T/4<t<5T/4) – The analytical calculation of power dissipation in this interval is analogous to that presented in the previous one. In fact, the steady state has been reached. Then, this deduction will be suppressed.

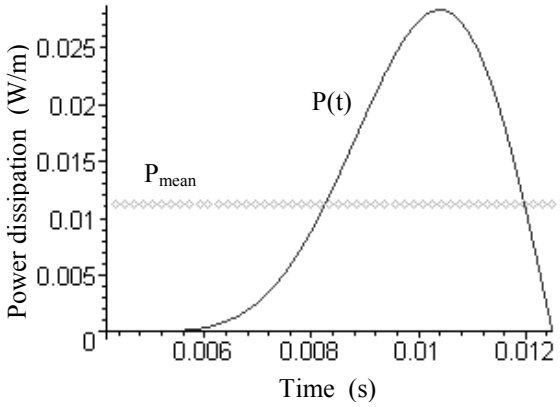

Fig.5. Power dissipation and its mean value for a sinusoidal current with effective value of 50 A and 60 Hz frequency, flowing in a superconductor cylinder with 3.6 mm radius and current density of 400 A/cm^2 (T/4<t<3T/4).

B. Numerical Simulation

A numerical solution is done to allow a better visualization of the electromagnetic behavior of the superconductor tube and ensure that the algorithm developed is correct. After this verification, the algorithm, with some modifications, can be used to model the influence of magnetic field and temperature variations.

For the numerical simulation, the cylinder is divided into cylindrical concentric skins. All electromagnetic variables are constants in each one. Figure 6 represents this division of the cylinder.

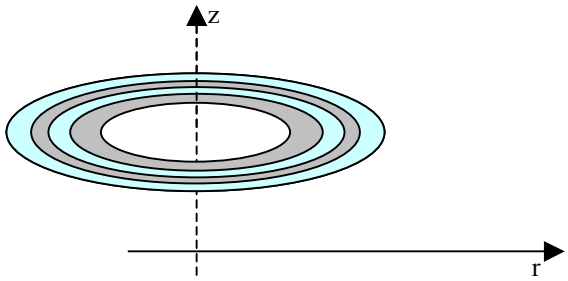

Fig.6. Division in skins of a superconductor cylinder for numerical simulation.

The algorithm developed is divided in these steps:

1- Input of simulation parameters;
2- Instantaneous current calculation;
3- Calculation of outmost magnetic field;
4- Application of current density at the analyzed skin;
5- Calculation of magnetic field with Amperè law, discounting the current flowing outside the analyzed skin;
6- Verification if with the current density application (step 4) the instantaneous current is reached. If the condition is true, go to step 7. If condition is false, jump to the inner adjoining skin and go back to step 4;
7- Electric field and power loss calculation. Increment the time value, until the final time defined is reached;
8- Graphics drawing.

The results of numerical simulation are graphically presented from Fig.7 to Fig.11.

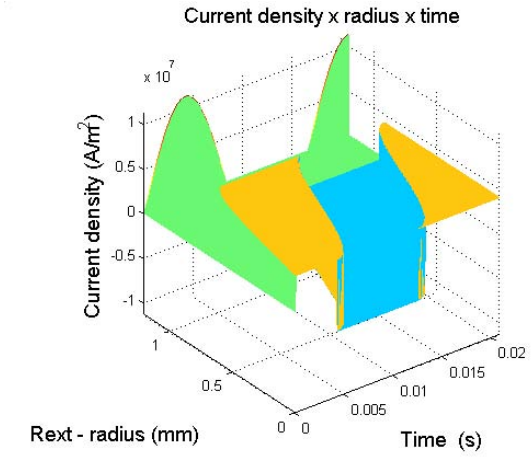

Fig.7. Current density for a sinusoidal current with effective value 50 A and 60 Hz, flowing in a superconductor cylinder with 3.6 mm radius and current density of 400 A/cm^2, simulation time 5T/4. The applied current multiplied by a constant as reference is inserted at the inner radius presented.

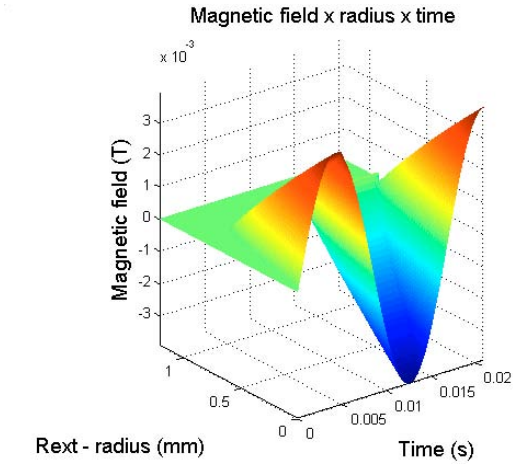

Fig.8. Magnetic field for the same parameters presented in Fig.7.

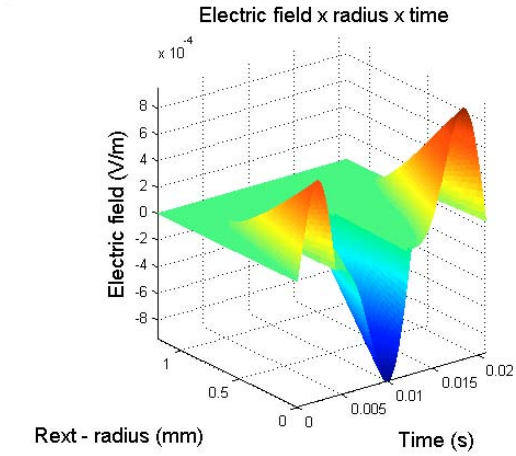

Fig.9. Electric field for the same parameters presented in Fig.7.

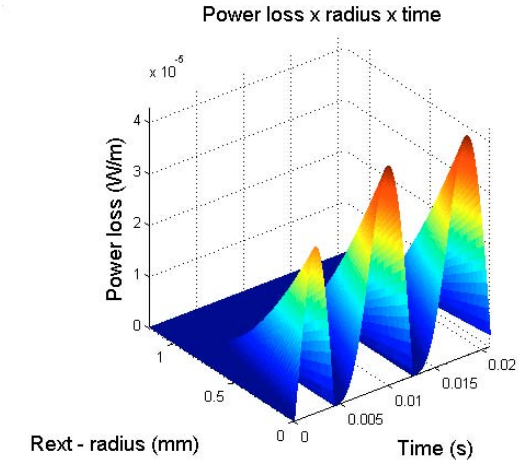

Fig.10. Power loss for the same parameters presented in Fig.7.

It can be seen in Fig.11 that the steady state is reached at T/4. As the results obtained with the numerical method (Fig. 11) agree with the analytical ones (Figs. 3 and 5) the algorithm developed can be considered validated.

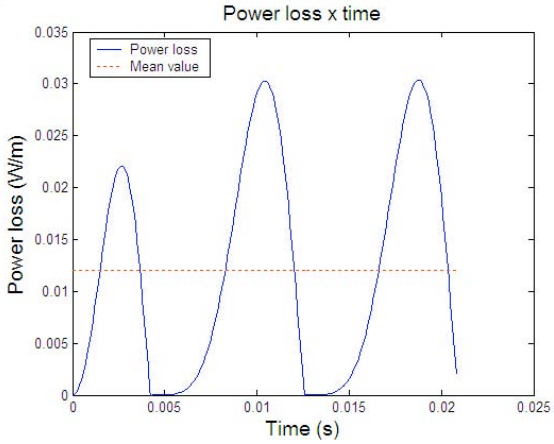

Fig.11. Total power loss for the same parameters presented in Fig.7.

C. Magnetic Field Influence

To model the influence of the magnetic field in the behavior of the superconductor tube the Kim model [7] is applied at the fourth step of the algorithm.

Instead of using a constant value of current density, the value used is presented in (10).

$$J(B) = \frac{J_C}{1 + \alpha B} \tag{10}$$

According to equation (10), the current density decreases with the growing of the magnetic field. This effect can be observed in Fig.12 and Fig. 13.

Using the same parameters presented in Fig. 7 and α estimated with experimental data from [8], the power loss obtained is 4.74 % greater then that one obtained without considering the magnetic field influence.

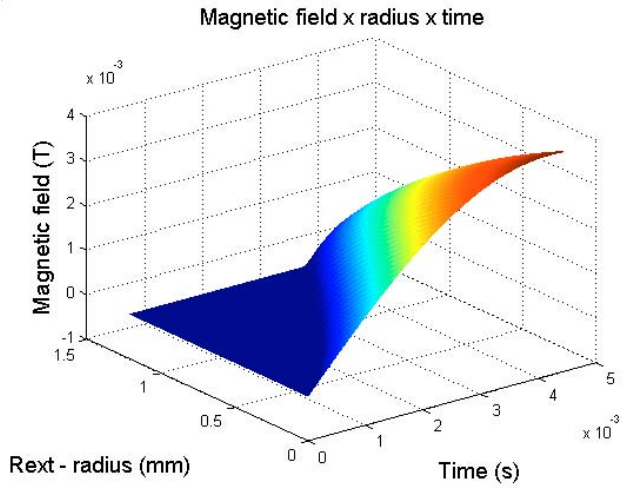

Fig.12. Magnetic field for the same parameters presented in Fig.7 and $\alpha = 200$.

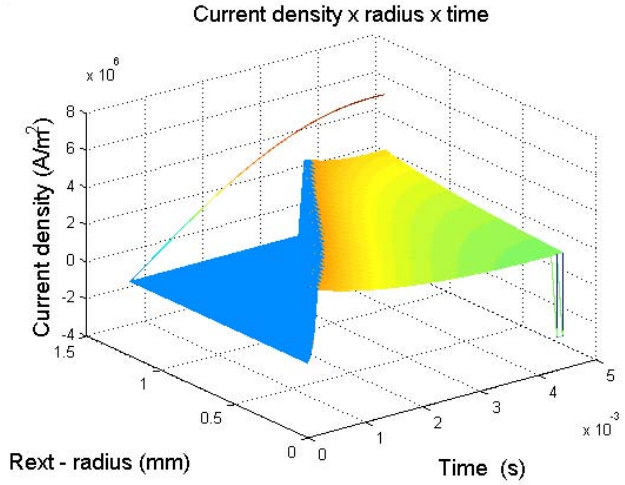

Fig.13. Current density the same parameters presented in Fig.7 and $\alpha = 200$ (to stand out that where the magnetic field is greater, the current density decreases).

D. Temperature Influence

The dependence of the current density and the temperature can be fitted by the linear function (11) [9].

$$J_C(T) = J_C(77K)\left(\alpha_{1T}.T + \alpha_{2T}\right) \tag{11}$$

In the seventh step of the algorithm, the energy dissipated ΔE by the superconductor is the product of the power loss by the step time of the simulation. Considering the superconductor in an adiabatic system, the temperature variation ΔT is defined by (12)

$$\Delta T = \frac{\Delta E}{C_T} \tag{12}$$

where C_T is the thermal capacity of the system.

Defining an initial temperature and using the current density obtained by (11) at the fourth step of the algorithm with the temperature calculated with (12), the influence of the temperature is modeled. The maximum temperature of the system is limited at the nitrogen liquid vaporization.

Using the same parameters of Fig. 7, initial temperature of 20 K and α_{1T} and α_{2T} estimated with experimental data from [8], the temperature variation and power dissipation are presented in Fig. 14 and Fig. 15.

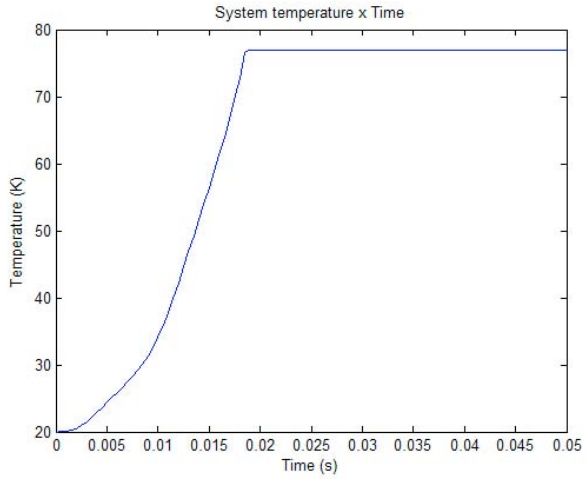

Fig.14. Temperature variation of the superconductor system, limited in 77 K.

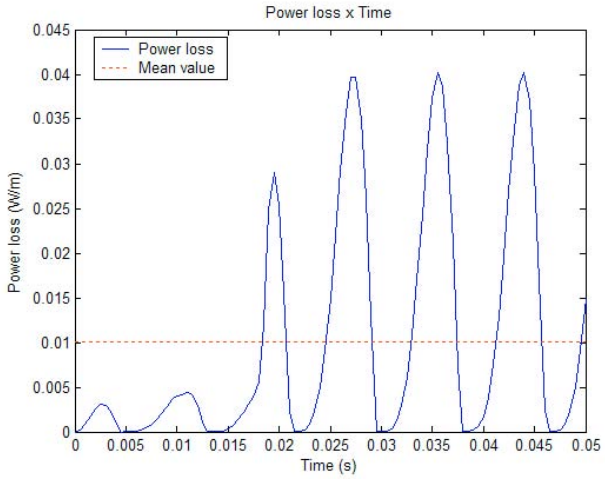

Fig.15. Total power loss and its mean value. The superconductor is more efficient in lowers temperatures.

III. CONCLUSION

The calculation of the loss dissipation of a RSFCL is essential in its design. Knowing this value, the limiter efficiency is determined and also the refrigeration equipment can be dimensioned.

With some changes in the algorithm, the influence of temperature or magnetic field in the current density can be implemented. This influence can not be analytically deduced and must be considered in the design of the limiter.

In this paper, a long cylinder was considered. To design a real RSFCL, a multiphysical numerical simulation (as the

finite element method) is indicated to determine the optimal geometry.

ACKNOWLEDGEMENT

The authors would like to acknowledge INB – Indústrias Nucleares do Brasil S.A - for the support given to this work.

REFERENCES

[1] E. Leung, 1997, "Surge protection for power grids", *IEEE Spectrum*, pp. 26-30, Jul. 1997.

[2] E. Calixte, Y. Yokomizu, H. Shimizu, et al, "Reduction of rating required for circuit breakeres by employing series-connected fault current limiters", *IEE Proc.-Gener. Transm. Distrib.*, v. 151, n. 1, pp. 36-42, Jan. 2004.

[3] M. Chen, W. Paul, M. Lakner, et al, "6.4 MVA resistive fault current limiter based on Bi-2212 superconductor", *Physica C*, pp. 1657-1663, 2002.

[4] C. P. Bean, "Magnetization of High-Field Superconductors", *Reviews of Modern Physics*, pp. 31-39, Jan. 1964.

[5] M. N. Wilson, *Superconducting Magnets*, New York, Oxford University Press Inc., 1983.

[6] Y. V. Bugoslavsky, "Magnetic measurements of critical current density, pinning and flux creep", In: CARDWELL, D. A., GINLEY, D. S., (eds), *Handbook of Superconducting Materials Volume II: Characterization, Applications and Cryogenics*, chapter D2.4, London, UK, IOP Publishing Ltd, 2003.

[7] KIM, Y. B., HEMPSTEAD, C. F., STRNAD, A. R., "Critical persistent currents in hard superconductors", *Physical Review Letters*, v. 9, n. 7, pp. 306-309, Oct. 1962

[8] CAN Superconductors, http://www.can.cz/leads.php, Mar. 2006

[9] BOCK, J., BREUER, F., WALTER, H., et al, "CURL 10: Development and Field-Test of a 10 kV/10 MVA Resistive Current Limiter Based on Bulk MCP-BSCCO 2212", *IEEE Transaction on Applied Superconductivity*, v. 15, n. 2, pp. 1955-1960, Jun. 2005